

The $a_1(1260)$ -meson longitudinal leading-twist distribution amplitude and the semileptonic decays $D \rightarrow a_1(1260)\ell^+\nu_\ell$ within the QCD sum rules

Dan-Dan Hu, Hai-Bing Fu*,[†] Tao Zhong,[‡] and Zai-Hui Wu
Department of Physics, Guizhou Minzu University, Guiyang 550025, P.R.China

Xing-Gang Wu[§]
*Department of Physics, Chongqing University, Chongqing 401331, P.R. China and
 Chongqing Key Laboratory for Strongly Coupled Physics, Chongqing 401331, P.R. China*
 (Dated: July 7, 2021)

In this paper, we make a detailed study on the axial-vector $a_1(1260)$ -meson longitudinal leading-twist distribution amplitude $\phi_{2;a_1}^\parallel(x, \mu)$ by using the QCD sum rules approach under the background field theory. By taking both the nonperturbative condensates up to dimension-six and the perturbative part up to next-to-leading order QCD corrections, its first three moments at the scale $\mu_0 = 1$ GeV are $\langle \xi_{2;a_1}^{\parallel;2} \rangle|_{\mu_0} = 0.210 \pm 0.018$, $\langle \xi_{2;a_1}^{\parallel;4} \rangle|_{\mu_0} = 0.091 \pm 0.007$, and $\langle \xi_{2;a_1}^{\parallel;6} \rangle|_{\mu_0} = 0.052 \pm 0.004$, respectively. Next, we calculate the transition form factors (TFFs) for $D \rightarrow a_1(1260)$ under the light-cone sum rules approach. At the large recoil region, we obtain $A(0) = 0.130^{+0.013}_{-0.015}$, $V_1(0) = 1.899^{+0.119}_{-0.127}$, $V_2(0) = 0.211^{+0.018}_{-0.020}$, and $V_0(0) = 0.235^{+0.026}_{-0.025}$. After extrapolating those TFFs into the physically allowable region, we obtain the differential decay widths and branching fractions of the semileptonic decays $D^{0(+)} \rightarrow a_1^{-(0)}(1260)\ell^+\nu_\ell$, i.e. $\mathcal{B}(D^0 \rightarrow a_1^-(1260)e^+\nu_e) = (5.421^{+0.702}_{-0.697}) \times 10^{-5}$, $\mathcal{B}(D^+ \rightarrow a_1^0(1260)e^+\nu_e) = (6.875^{+0.890}_{-0.884}) \times 10^{-5}$, $\mathcal{B}(D^0 \rightarrow a_1^-(1260)\mu^+\nu_\mu) = (4.864^{+0.647}_{-0.641}) \times 10^{-5}$, $\mathcal{B}(D^+ \rightarrow a_1^0(1260)\mu^+\nu_\mu) = (6.169^{+0.813}_{-0.821}) \times 10^{-5}$.

PACS numbers: 13.25.Hw, 11.55.Hx, 12.38.Aw, 14.40.Be

I. INTRODUCTION

Extensive studies on the semileptonic decays of D -meson into axial-vector meson are important for understanding the non-perturbative effects in weak interactions. In the constituent quark model, the quantum number of a meson is determined by the quantum number of constituent quarks. The meson with quantum state $J^P = 1^+$ is called an axial-vector meson. There are two types of axial-vector meson, one has the quantum state $J^{PC} = 1^{+-}$, denoted as the 1P_1 state; and the other one has the quantum state $J^{PC} = 1^{++}$, denoted as the 3P_1 state. Among the axial-vector mesons, it is usually thought that only the isospin triplet heavy state mesons $b_1(1235)$ and $a_1(1260)$ do not have a mixing phenomenon. Thus their internal structures are relatively clear. For example, the observation of the charmless hadronic decay processes involving $a_1(1260)$ -meson, such as $B^0 \rightarrow a_1^\pm(1260)\pi^\mp$, measured by the BABAR and Belle collaborations [1–5], indicate that $a_1(1260)$ is in 3P_1 state. Those measurements help investigate the production mechanism of axial-vectors via hadronic decay processes and for probing the structures of axial-vector mesons. Thus it is important to give a detailed theoretical study on the semileptonic decay $D \rightarrow a_1(1260)\ell^+\nu_\ell$.

The transition form factors (TFFs) of $D \rightarrow a_1(1260)$

are key components for investigating the semileptonic decays involving $a_1(1260)$. The heavy-to-light axial-vector meson TFFs have been calculated under various approaches, such as the QCD sum rules (QCDSR) [6], the covariant light-front quark model (CLFQM) [7], the constituent quark model (CQM) [8], the light-cone sum rules (LCSR) [9–13], the perturbative QCD (PQCD) [14–16], and the three-point QCD sum rules (3PSR) [17]. The LCSR approach is one of the effective tools in determining non-perturbative parameters of hadronic states. By using the LCSR approach, one carries out the operator product expansion (OPE) near the light-cone $x^2 \approx 0$, and the nonperturbative hadronic matrix elements are parameterized by the light-cone distribution amplitudes (LCDAs) with various twists. In this paper, we shall adopt the LCSR approach to deal with the $D \rightarrow a_1(1260)$ TFFs by using a left-handed chiral current, which highlights the longitudinal leading twist LCDA contribution and greatly suppresses the higher-twist contributions.

The longitudinal twist-2 LCDA $\phi_{2;a_1}^\parallel(x, \mu)$ of $a_1(1260)$ at the scale μ can be expanded as Gegenbauer series

$$\phi_{2;a_1}^\parallel(x, \mu) = 6x\bar{x} \left(1 + \sum_n a_{n;a_1}^\parallel(\mu) C_n^{3/2}(\xi) \right), \quad (1)$$

where $\xi = (2x - 1)$ and $\bar{x} = (1 - x)$. $a_{n;a_1}^\parallel(\mu)$ are Gegenbauer moments, and at present, its first one has been calculated in [11, 12], i.e. $a_{2;a_1}^\parallel(\mu_0 = 1\text{GeV}) = -0.02 \pm 0.02$.

In the paper, we shall calculate the moments $a_{n;a_1}^\parallel(\mu)$ by using the QCDSR approach under the background field theory [18] (BFTSR). The approach BFTSR have been widely used in calculating the twist-2 or twist-3

*Corresponding author

[†]Electronic address: fuhb@cqu.edu.cn

[‡]Electronic address: zhongtao1219@sina.com

[§]Electronic address: wuxg@cqu.edu.cn

LCDAs of the heavy and light mesons [19–30]. Within the BFTSR framework, the quark and gluon fields are consisted by the background fields and their surrounding quantum fluctuations, and the usual vacuum condensates are described by the classical background fields. The BFTSR provides a clear picture for the bound-state internal structures, and makes the sum rule calculation more simplified.

The rest of the paper are organized as follows. In Sec. II, we present the basic idea of the BFTSR, give the calculated Gegenbauer moments of $\phi_{2;a_1}^{\parallel}(x, \mu)$ and provide the formulas for the branching fractions and TFFs for the semileptonic decays $D \rightarrow a_1(1260)\ell^+\nu_\ell$. In Sec. III, we present our numerical results and make a comparison with experimental measurements and theoretical predictions. Sections IV is reserved for a summary.

II. CALCULATION TECHNOLOGY

The QCD Lagrangian

$$\mathcal{L}_{\text{QCD}}(\mathcal{A}, \psi) = -\frac{1}{4}G_{\mu\nu}^a G^{a\mu\nu} + \bar{\psi}(i\not{D} - m)\psi, \quad (2)$$

where $G_{\mu\nu}^a = \partial_\mu \mathcal{A}_\nu^a - \partial_\nu \mathcal{A}_\mu^a + g_s f^{abc} \mathcal{A}_\nu^b \mathcal{A}_\mu^c$ with $a, b, c = (1, 2, \dots, 8)$ stands for the gluon field strength tensor, g_s is the strong coupling constant, f^{abc} is the structure constant of the $\text{SU}_f(3)$ -group. The gluon field and quark field satisfy the QCD equation of motion

$$(i\not{D} - m)\psi(x) = 0 \quad (3)$$

$$\tilde{D}_\mu^{ab} G^{b\nu\mu}(x) = g_s \bar{\psi}(x) \gamma^\nu T^a \psi(x) \quad (4)$$

where $D_\mu = \partial_\mu - ig_s T^a \mathcal{A}_\mu^a$ and $\tilde{D}_\mu^{ab} = \delta^{ab} \partial_\mu - g_s f^{abc} \mathcal{A}_\mu^c$ are fundamental and adjoint representations of the gauge covariant derivatives respectively.

The basic idea of background field theory is one can use the classical background field to describe the non-perturbative effects which satisfied the theoretical equation of motion, and use the quantum field to describe the perturbative parts, i.e. so-called the quantum fluctuation. So the gluon field $\mathcal{A}_\mu^a(x)$ and quark field $\psi(x)$ in the QCD Lagrangian or Green function make the following substitution [18, 31, 32]

$$\mathcal{A}_\mu^a(x) \rightarrow \mathcal{A}_\mu^a(x) + \phi_\mu^a(x), \quad (5)$$

$$\psi(x) \rightarrow \psi(x) + \eta(x). \quad (6)$$

where in the right hand side of the arrow, $\mathcal{A}_\mu^a(x)$ with $a = 1, \dots, 8$ and $\psi(x)$ indicate the background fields of the gluon and quark, respectively, $\phi_\mu^a(x)$ and $\eta(x)$ stand for the gluon and quark quantum fields, i.e. the quantum fluctuation on the background fields and about the corresponding Feynman rule of BFT can be found in Ref. [18]. According to the equivalent Laplace density, we can get the equations satisfied by quarks and gluon propagators in BFTSR [26].

$$(i\not{D}(\mathcal{A}) - m)S_F(x, 0) = \delta^4(x), \quad (7)$$

$$[g^{\mu\nu}(\tilde{D}^2)^{ab} + 2f^{abc}G^{c\mu\nu}]S_{\nu,p}^{bd}(x, 0) = \delta^{ad}g_p^\mu \delta^4(x) \quad (8)$$

After using the Eqs. (7) and (8) and employ the fixed-point gauge, i.e. $x^\mu \mathcal{A}_\mu^a(x) = 0$, we can get the expressions for quark and gluon propagators up to dimension-six completely [30].

Considering the definition

$$\begin{aligned} &\langle 0|\bar{d}(0)\not{z}\gamma_5(iz \cdot \overleftrightarrow{D})^n u(0)|a_1(q, \lambda)\rangle \\ &= i(z \cdot q)^{n+1}(e^{*(\lambda)} \cdot z)m_{a_1}f_{a_1}^{\parallel}\langle \xi_{2;a_1}^{n;\parallel}\rangle|_\mu, \end{aligned} \quad (9)$$

where $f_{a_1}^{\parallel}$ is the $a_1(1260)$ -meson decay constant, q and $e^{*(\lambda)}$ are momentum and polarization vector of the $a_1(1260)$ -meson. The polarization vector satisfies the relationship $(e^{*(\lambda)} \cdot z) \approx 1$ [33]. And the covariant derivative have the relation $(iz \cdot \overleftrightarrow{D})^n = (iz \cdot \overrightarrow{D} - iz \cdot \overleftarrow{D})^n$. As a special case, the 0th-order Gegenbauer moment satisfies the normalization condition

$$\langle \xi_{2;a_1}^{\parallel;0}\rangle|_\mu = \int_0^1 du \phi_{2;a_1}^{\parallel}(u, \mu) = 1 \quad (10)$$

To derive the sum rules for the moments $\langle \xi_{2;a_1}^{\parallel;n}\rangle|_\mu$, we introduce the following correlation function,

$$\begin{aligned} \Pi_{2;a_1}^{(n,0)}(z, q) &= i \int d^4x e^{iq \cdot x} \langle 0|T\{J_n(x), J_0^\dagger(0)\}|0\rangle \\ &= (z \cdot q)^{n+2} I_{2;a_1}^{(n,0)}(q^2), \end{aligned} \quad (11)$$

where $J_n(x) = \bar{d}(x)\not{z}\gamma_5(iz \cdot \overleftrightarrow{D})^n u(x)$, $J_0^\dagger(0) = \bar{u}(0)\not{z}\gamma_5 d(0)$ and $z^2 \rightsquigarrow 0$. Due to the G -parity, the leading twist LCDA $\phi_{2;a_1}^{\parallel}(x, \mu)$ of a $a_1(1260)$ -meson for 3P_1 state defined by the nonlocal axial-vector current is symmetric, which means only even moments are non-zero, i.e. $n = (0, 2, 4, 6, \dots)$. In deep Euclidean region $q^2 \ll 0$, one can apply the OPE for the correlation function Eq. (11). Based on BFTSR, let the replacement rules Eqs. (5) and (6) into the correlation Eq. (11), we obtain

$$\begin{aligned} \Pi_{2;a_1}^{(n,0)}(z, q) &= i \int d^4x e^{iq \cdot x} \{ \\ &\quad - \text{Tr}\langle 0|S_F^s(0, x)\not{z}\gamma_5(iz \cdot \overleftrightarrow{D})^n S_F^s(x, 0)\not{z}\gamma_5|0\rangle \\ &\quad + \text{Tr}\langle 0|\bar{d}(x)u(0)\not{z}\gamma_5(iz \cdot \overleftrightarrow{D})^n S_F^s(x, 0)\not{z}\gamma_5|0\rangle \\ &\quad + \text{Tr}\langle 0|S_F^s(0, x)\not{z}\gamma_5(iz \cdot \overleftrightarrow{D})^n \bar{d}(0)u(x)\not{z}\gamma_5|0\rangle \\ &\quad + \dots \}. \end{aligned} \quad (12)$$

And the coefficients before the operators can be calculated perturbatively. Lorentz invariant scalar function $\Pi_{2;a_1}^{(n,0)}(q^2)$ in Eq. (11) depends on the condensation parameter and will encounter the vacuum matrix element which can be found in Ref. [19].

By inserting a complete set of intermediated hadronic states into the correlator Eq. (11), we obtain

$$\text{Im}I_{2;a_1, \text{Had}}^{(n,0)}(q^2) = \pi \delta(q^2 - m_{a_1}^2) f_{a_1}^2 m_{a_1}^2 \langle \xi_{2;a_1}^{\parallel;n}\rangle|_\mu$$

$$+ \pi \frac{3}{4\pi^2(n+1)(n+3)} \theta(q^2 - s_{a_1}), \quad (13)$$

in which s_{a_1} stands for the continuum threshold. The first term is the contribution of $a_1(1260)$ -meson ground state, and the second term is the contribution of continuum states above the ground state. According to the dispersion relation of the invariant function $I_{2;a_1}^{(n,0)}(q^2)$ and its the QCD OPE, we can obtain the sum rule

$$\frac{1}{\pi} \int_0^\infty ds \frac{\text{Im} I_{2;a_1}^{(n,0)}(s)}{s - q^2} = I_{2;a_1, \text{QCD}}^{(n,0)}(q^2) \quad (14)$$

The Borel transform helps to depress the contribution

of the continuum state on the left of Eq. (14) and the contribution of the high dimensional aggregation on the right, and finally the sum rule is obtained

$$\frac{1}{\pi} \frac{1}{M^2} \int ds e^{-s/M^2} \text{Im} I_{a_1, \text{had}}^{(n,0)}(s) = \hat{\mathcal{B}}_{M^2} I_{2;a_1, \text{QCD}}^{(n,0)}(q^2), \quad (15)$$

where M^2 is Borel parameter coming from the Borel transformation. By following standard sum rules processes [18, 19, 34–38], we can obtain the expression of the moment of $a_1(1260)$ -meson longitudinal twist-2 LCDA:

$$\begin{aligned} \frac{f_{a_1}^2 m_{a_1}^2 \langle \xi_{2;a_1}^{\parallel;n} \rangle |_\mu \langle \xi_{2;a_1}^{\parallel;0} \rangle |_\mu}{M^2 e^{m_{a_1}^2/M^2}} &= \frac{3}{4\pi^2(n+1)(n+3)} \left(1 + \frac{\alpha_s}{\pi} A'_n \right) (1 - e^{-s_{a_1}/M^2}) + \frac{(m_u + m_d) \langle \bar{q}q \rangle}{M^4} + \frac{\langle \alpha_s G^2 \rangle}{12\pi M^4} \frac{1 + n\theta(n-2)}{n+1} \\ &- \frac{8n+1}{18} \frac{(m_u + m_d) \langle g_s \bar{q} \sigma T G q \rangle}{M^6} + \frac{\langle g_s \bar{q}q \rangle}{81 M^6} 4(2n+1) - \frac{\langle g_s^3 f G^3 \rangle}{48\pi^2 M^6} n\theta(n-2) + \frac{\langle g_s^2 \bar{q}q \rangle^2}{M^6} \frac{2 + \kappa^2}{486\pi^2} \\ &\times \left\{ -2(51n+25) \left(-\ln \frac{M^2}{\mu^2} \right) + 3(17n+35) + \theta(n-2) \left[2n \left(-\ln \frac{M^2}{\mu^2} \right) - 25(2n+1) \tilde{\psi}(n) \right. \right. \\ &\left. \left. + \frac{1}{n} (49n^2 + 100n + 56) \right] \right\}. \end{aligned} \quad (16)$$

In which the function $\tilde{\psi}(n) = \psi((n+1)/2) - \psi(n/2) + \ln 4$. The values of NLO correction are $A'_0 = 0$, $A'_2 = 5/3$, $A'_4 = 59/127$, $A'_6 = 353/135$. When taking $n = 0$, the sum rule of the 0th-order moment of DA is obtained as:

$$\begin{aligned} \frac{(\langle \xi_{2;a_1}^{\parallel;0} \rangle |_\mu)^2 f_{a_1}^2 m_{a_1}^2}{M^2 e^{m_{a_1}^2/M^2}} &= \frac{1}{4\pi^2} (1 - e^{-s_{a_1}/M^2}) + \frac{(m_u + m_d) \langle \bar{q}q \rangle}{M^4} + \frac{\langle \alpha_s G^2 \rangle}{12\pi M^4} - \frac{(m_u + m_d) \langle g_s \bar{q} \sigma T G q \rangle}{18 M^6} + \frac{4 \langle g_s q \bar{q} \rangle^2}{81 M^6} + \frac{\langle g_s^2 \bar{q}q \rangle^2}{M^6} \\ &\times \frac{2 + \kappa^2}{486\pi^2} \left[-50 \left(-\ln \frac{M^2}{\mu^2} \right) + 105 \right] \end{aligned} \quad (17)$$

In order to further consider the impact of the sum rule of $\langle \xi_{2;a_1}^{\parallel;0} \rangle |_\mu$ in the full Borel parameter regions, we will use the equation

$$\langle \xi_{2;a_1}^{\parallel;n} \rangle |_\mu = \frac{\langle \xi_{2;a_1}^{\parallel;n} \rangle |_\mu \langle \xi_{2;a_1}^{\parallel;0} \rangle |_\mu}{\sqrt{(\langle \xi_{2;a_1}^{\parallel;0} \rangle |_\mu)^2}}, \quad (18)$$

to obtain more accurate moments $\langle \xi_{2;a_1}^{\parallel;n} \rangle |_\mu$ [39]. By using the resultant moments $\langle \xi_{2;a_1}^{\parallel;n} \rangle |_\mu$, we can obtain the Gegenbauer moments $a_{2;a_1}^{\parallel;n}(\mu)$ up to 6th-order by using the following relations,

$$\begin{aligned} \langle \xi_{2;a_1}^{\parallel;2} \rangle |_\mu &= \frac{1}{5} + \frac{12}{35} a_{2;a_1}^{\parallel;2}(\mu), \\ \langle \xi_{2;a_1}^{\parallel;4} \rangle |_\mu &= \frac{3}{35} + \frac{8}{35} a_{2;a_1}^{\parallel;2}(\mu) + \frac{8}{77} a_{2;a_1}^{\parallel;4}(\mu), \\ \langle \xi_{2;a_1}^{\parallel;6} \rangle |_\mu &= \frac{1}{21} + \frac{12}{77} a_{2;a_1}^{\parallel;2}(\mu) + \frac{120}{1001} a_{2;a_1}^{\parallel;4}(\mu) \end{aligned}$$

$$+ \frac{64}{2145} a_{2;a_1}^{\parallel;6}(\mu). \quad (19)$$

Those relations are obtained by applying the Gegenbauer polynomial expansion of $\phi_{2;a_1}^{\parallel}(x, \mu)$.

In order to derive the LCSR for the $D \rightarrow a_1(1260)$ TFFs, we suggest to start from the following chiral correlation function

$$\begin{aligned} \Pi_\mu(p, q) &= i \int d^4x e^{iq \cdot x} \langle a_1(p, \lambda) | T \{ j_\mu(x), j_D^\dagger(0) \} | 0 \rangle \\ &= -\Pi_1 e_\mu^{*(\lambda)} + \Pi_2 (e^{*(\lambda)} \cdot q) (2p + q)_\mu \\ &\quad + \Pi_3 (e^{*(\lambda)} \cdot q) q_\mu + i \Pi_V \epsilon_\mu^{\alpha\beta\gamma} e_\alpha^{*(\lambda)} q_\beta p_\gamma, \end{aligned} \quad (20)$$

with $j_\mu(x) = \bar{d}(x) \gamma_\mu (1 - \gamma_5) c(x)$ and $j_D^\dagger(x) = i \bar{c}(x) (1 - \gamma_5) u(x)$. In the time-like q^2 -region, the long distance quark-gluon interactions become important. To deal with the correlation function in the time-like region, one can insert a complete set of the intermediate hadronic

states with the same quantum numbers to obtain the hadronic expression. By isolating the pole term of the pseudoscalar D -meson, we obtain

$$\Pi_\mu^H(p, q) = \frac{\langle a_1 | \bar{d} \gamma_\mu (1 - \gamma_5) c | D \rangle \langle D | \bar{c} i \gamma_5 q | 0 \rangle}{m_D^2 - (p + q)^2} + \sum_H \frac{\langle a_1 | d \gamma_\mu (1 - \gamma_5) c | D^H \rangle \langle D^H | \bar{c} i (1 - \gamma_5) q | 0 \rangle}{m_D^H - (p + q)^2}, \quad (21)$$

with the matrix element $\langle D | \bar{c} i \gamma_5 q | 0 \rangle = m_D^2 f_D / m_c$. The $D \rightarrow a_1(1260)$ transition matrix elements have the expression [15]:

$$\langle a_1(p, \lambda) | d \gamma_\mu \gamma_5 c | D(p + q) \rangle = -\epsilon^{\mu\nu\alpha\beta} e_\nu^{*(\lambda)} q_\alpha p_\beta \frac{2iA(q^2)}{m_D - m_{a_1}} \quad (22)$$

$$\begin{aligned} \langle a_1(p, \lambda) | d \gamma_\mu c | D(p + q) \rangle &= -e_\mu^{*(\lambda)} (m_D - m_{a_1}) V_1(q^2) \\ &+ (2p + q)_\mu \frac{e^{*(\lambda)} \cdot q}{m_D - m_{a_1}} V_2(q^2) + q_\mu (e^{*(\lambda)} \cdot q) \frac{2m_{a_1}}{q^2} \\ &\times [V_3(q^2) - V_0(q^2)] \end{aligned} \quad (23)$$

Where $e^{*(\lambda)}$ stands for $a_1(1260)$ -meson polarization vector with $\lambda = (\perp, \parallel)$ being its transverse or longitudinal component respectively. Momentum p is of the $a_1(1260)$ -meson and $q = p_D - p_{a_1}$ is the momentum transfer between the two mesons, which followed the linear relationships:

$$V_3(q^2) = \frac{(m_D - m_{a_1})}{2m_{a_1}} V_1(q^2) - \frac{(m_D + m_{a_1})}{2m_{a_1}} V_2(q^2) \quad (24)$$

$$V_0(q^2) = V_3(q^2) + \frac{q^2}{2m_{a_1}(m_D - m_{a_1})} V_2(q^2) \quad (25)$$

Thus, the hadronic expression for invariant amplitudes $\Pi_{1,2,3,4}^H[q^2, (p + q)^2]$ are

$$\begin{aligned} \Pi_1^H[q^2, (p + q)^2] &= \frac{m_D^2 f_D (m_D - m_{a_1})}{m_c [m_D^2 - (p + q)^2]} V_1(q^2) \\ &+ \int_{s_0}^\infty \frac{\rho_1^{\text{had}}}{s - (p + q)^2} ds + \text{subtractions} \\ \Pi_2^H[q^2, (p + q)^2] &= \frac{m_D^2 f_D}{m_c (m_D - m_{a_1}) [m_D^2 - (p + q)^2]} \end{aligned} \quad (26)$$

$$\times V_2(q^2) + \int_{s_0}^\infty \frac{\rho_2^{\text{had}}}{s - (p + q)^2} ds + \text{subtractions} \quad (27)$$

$$\begin{aligned} \Pi_3^H[q^2, (p + q)^2] &= \frac{1}{q^2} \frac{2m_{a_1} m_D^2 f_D}{m_c [m_D^2 - (p + q)^2]} [V_3(q^2) \\ &- V_0(q^2)] + \int_{s_0}^\infty \frac{\rho_3^{\text{had}}}{s - (p + q)^2} ds + \text{subtractions} \end{aligned} \quad (28)$$

$$\begin{aligned} \Pi_4^H[q^2, (p + q)^2] &= \frac{2m_D^2 f_D}{(m_D - m_{a_1}) m_c [m_D^2 - (p + q)^2]} \\ &\times A(q^2) + \int_{s_0}^\infty \frac{\rho_4^{\text{had}}}{s - (p + q)^2} ds + \text{subtractions} \end{aligned} \quad (29)$$

Here we have replaced the contributions of the higher resonances and the continuum states by the dispersion integrations. The continuum threshold parameter s_0 is set as the value near the squared mass of the lowest scalar D -meson. The spectral densities $\rho_{1,2,3,4}^{\text{had}}$ can be approximated by applying the conventional quark-hadron duality ansatz

$$\rho_{1,2,3,4}^{\text{had}} = \rho_{1,2,3,4}^{\text{QCD}} \theta(s - s_0) \quad (30)$$

On the other hand, within in the space-like region, we can calculate the correlation via the QCD theory. In this region, the correlation can be treated by the OPE with the coefficients being pQCD calculated. To calculate the correlation function we need to know the expression for the c -quark propagator

$$\begin{aligned} \langle 0 | T \{ c(x) \bar{c}(0) \} | 0 \rangle &= i \int \frac{d^4 k}{(2\pi)^4} e^{-ik \cdot x} \frac{m_c + \not{k}}{m_c^2 - k^2} - i g_s \\ &\times \int \frac{d^4 k}{(2\pi)^4} e^{-ik \cdot x} \int_0^1 dv \left[\frac{m_c + \not{k}}{2(m_c^2 - k^2)^2} G^{\mu\nu}(vx) \sigma_{\mu\nu} \right. \\ &\left. + \frac{v}{m_c^2 - k^2} x_\mu G^{\mu\nu}(vx) \gamma_\nu \right] \end{aligned} \quad (31)$$

The first term on the r.h.s corresponds to the free quark propagator. After applying the OPE to the correlation function, we obtain

$$\begin{aligned} \Pi_\mu^{\text{OPE}} &= -2im_c \int \frac{d^4 x d^4 k}{(2\pi)^4} e^{i(q-k)x} \left\{ \left[\frac{1}{m_c^2 - k^2} \langle a_1(p, \lambda) | \bar{d}(x) \gamma_\mu u(0) | 0 \rangle - \langle a_1(p, \lambda) | \bar{d}(x) \gamma_\mu \gamma_5 u(0) | 0 \rangle \right] \right. \\ &\left. - \int_0^1 dv \frac{1}{(m_c^2 - k^2)^2} \left[i g_{\mu\alpha} \langle a_1(p, \lambda) | \bar{d}(x) g_s G^{\alpha\beta}(\nu x) \gamma_\beta \gamma_5 u(0) | 0 \rangle + \langle a_1(p, \lambda) | \bar{d}(x) g_s \tilde{G}_{\mu\nu}(\nu x) \gamma^\nu u(0) | 0 \rangle \right] \right\} \end{aligned} \quad (32)$$

Additionally, in procedure of calculation, we also need to use the expression of matrix elements, which includes of the twist-2, 3, 4 LCDAs, which are listed in Appendix A. Due to the smallest contributions of the three-particle part, one

can ignored this part safely. After matching the correlation function within different regions with dispersion relation and applying the conventional Borel transformation, we can get the final TFFs within LCSR approach

$$V_1(q^2) = \frac{2m_c^2 m_{a_1} f_{a_1}}{m_D^2 f_D (m_D - m_{a_1})} \int_0^1 \frac{du}{u} e^{(m_D^2 - s(u))/M^2} \left[\Theta(c(u, s_0)) \phi_{3;a_1}^\perp(u) - \tilde{\Theta}(c(u, s_0)) \frac{m_{a_1}^2}{u M^2} \Psi_{4;a_1}^\parallel \right] + \frac{2m_c^2 m_{a_1}^2}{m_D^2 f_D} \\ \times \frac{f_{3;a_1}^V - f_{3;a_1}^A}{m_D - m_{a_1}} \int \mathcal{D}\alpha \int_0^1 dv e^{(m_D^2 - s(X))/M^2} \frac{1}{X^2 M^2} \Theta(c(X, s_0)) \left[\tilde{\Phi}_{3;a_1}^\parallel(\alpha) - \Phi_{3;a_1}^\parallel(\alpha) \right], \quad (33)$$

$$V_2(q^2) = \frac{2m_c^2 m_{a_1} f_{a_1} (m_D - m_{a_1})}{m_D^2 f_D} \int_0^1 \frac{du}{u} e^{(m_D^2 - s(u))/M^2} \left[\frac{1}{u M^2} \tilde{\Theta}(c(u, s_0)) \Phi_{2;a_1}^\parallel(u) + \frac{m_{a_1}^2}{u M^4} \tilde{\tilde{\Theta}}(c(u, s_0)) \Psi_{4;a_1}^\parallel(u) \right] \\ - \frac{m_c^2 m_{a_1}^2 (f_{3;a_1}^V - f_{3;a_1}^A) (m_D - m_{a_1})}{m_D^2 f_D} \int \mathcal{D}\alpha \int_0^1 dv e^{(m_D^2 - s(X))/M^2} \frac{1}{X^3 M^4} \Theta(c(X, s_0)) \left[\tilde{\Phi}_{3;a_1}^\parallel(\alpha) - \Phi_{3;a_1}^\parallel(\alpha) \right], \quad (34)$$

$$V_3(q^2) - V_0(q^2) = -\frac{q^2 m_c^2 f_{a_1}}{m_D^2 f_D} \int_0^1 \frac{du}{u} e^{(m_D^2 - s(u))/M^2} \left[\frac{1}{u M^2} \tilde{\Theta}(c(u, s_0)) \Phi_{2;a_1}^\parallel(u) - \frac{m_{a_1}^2 (2-u)}{u^2 M^4} \tilde{\tilde{\Theta}}(c(u, s_0)) \Psi_{4;a_1}^\parallel(u) \right] \\ + \frac{q^2 m_c^2 m_{a_1}^2 (f_{3;a_1}^V - f_{3;a_1}^A)}{m_D^2 f_D} \int \mathcal{D}\alpha \int_0^1 dv e^{(m_D^2 - s(X))/M^2} \frac{1}{X^3 M^4} \Theta(c(X, s_0)) \left[\tilde{\Phi}_{3;a_1}^\parallel(\alpha) - \Phi_{3;a_1}^\parallel(\alpha) \right], \quad (35)$$

$$A(q^2) = \frac{m_c^2 m_{a_1} f_{a_1} (m_D - m_{a_1})}{2m_D^2 f_D} \int_0^1 du e^{(m_D^2 - s(u))/M^2} \frac{1}{u^2 M^2} \tilde{\Theta}(c(u, s_0)) \psi_{3;a_1}^\perp(u). \quad (36)$$

Where

$$\Phi_{2;a_1}^\parallel(u) = \int_0^u dv \phi_{2;a_1}^\parallel(v), \\ \Phi_{3;a_1}^\perp(u) = \int_0^u dv \phi_{3;a_1}^\perp(v), \\ \Psi_{4;a_1}^\parallel(u) = \int_0^u dv \int_0^v dw \psi_{4;a_1}^\parallel(w).$$

Furthermore, The differential decay widths can be related with the parametrization of the transition matrix elements in terms of TFFs. The detail expression can be read off [15]

$$\frac{d\Gamma_L(D \rightarrow a_1(1260)\ell^+\nu_\ell)}{dq^2} = \left(\frac{q^2 - m_\ell^2}{q^2} \right)^2 \frac{\sqrt{\lambda} G_F^2 |V_{cd}|^2}{384\pi^3 m_D^3} \\ \times \frac{1}{q^2} \left[3m_\ell^2 \lambda V_0^2(q^2) + \frac{m_\ell^2 + 2q^2}{2m_{a_1}} \left| (m_D^2 - m_{a_1}^2 - q^2) \right. \right. \\ \left. \left. \times (m_D - m_{a_1}) V_1(q^2) - \frac{\lambda}{m_D - m_{a_1}} V_2(q^2) \right|^2 \right] \quad (37)$$

$$\frac{d\Gamma_\pm(D \rightarrow a_1(1260)\ell^+\nu_\ell)}{dq^2} = \left(\frac{q^2 - m_\ell^2}{q^2} \right)^2 \frac{\sqrt{\lambda} G_F^2 |V_{cd}|^2}{384\pi^3 m_D^3} \\ \times (m_\ell^2 + 2q^2) \lambda \left| \frac{A(q^2)}{m_D - m_{a_1}} \mp \frac{(m_D - m_{a_1}) V_1(q^2)}{\sqrt{\lambda}} \right|^2 \quad (38)$$

where G_F is Fermi coupling constant, $|V_{cd}|$ is CKM matrix element and $\lambda = (m_D^4 + m_{a_1}^4 + q^4 - 2m_{a_1}^2 m_D^2 -$

TABLE I: The standard for determining Borel windows, the Borel windows and the corresponding values of the $a_1(1260)$ -meson leading twist DA moments $\langle \xi_{2;a_1}^{\parallel;n} \rangle|_\mu$ at $s_{a_1} = 2.6(4)$ GeV. Where ‘‘Con.’’ represent the continuum state contribution and ‘‘Six.’’ represent the dimensional-six condensates contribution.

n	2	4	6
Con.	< 20%	< 25%	< 30%
Six.	< 5%	< 5%	< 5%
M^2	[1.782, 2.738]	[2.740, 3.629]	[3.669, 4.723]
$\langle \xi_{2;a_1}^{\parallel;n} \rangle _\mu$	[0.221, 0.196]	[0.094, 0.086]	[0.054, 0.049]

$2q^2 m_D^2 - 2q^2 m_{a_1}^2$), the $d\Gamma_L$ and $d\Gamma_T = d\Gamma_+ + d\Gamma_-$ are longitudinal and transverse components of the differential decay widths, respectively. The total differential decay widths are the sum of longitudinal and transverse parts, i.e. $d\Gamma_{\text{total}} = d\Gamma_L + d\Gamma_T$.

III. NUMERICAL ANALYSIS

A. Input parameters

We adopt the following parameters to do the numerical calculation. The current charm-quark mass, $\bar{m}_c(\bar{m}_c) = 1.27 \pm 0.02$ GeV, the D and $a_1(1260)$ -meson mass $m_{D^0} = 1.865$ GeV, $m_{D^+} = 1.870$ GeV and $m_{a_1} \approx 1.230$ GeV from the Particle Data Group (PDG) [40]. The D and $a_1(1260)$ -meson decay constants are taken

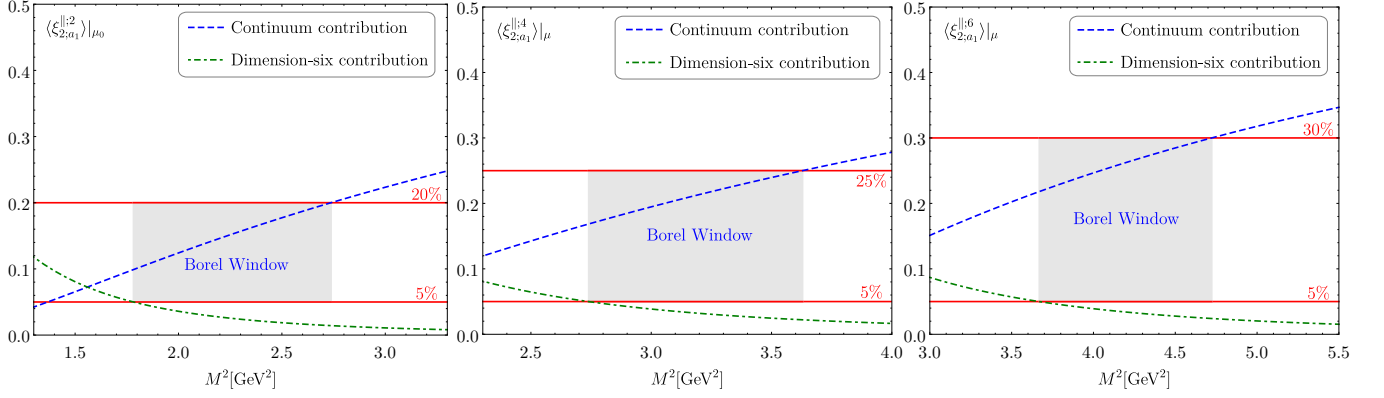


FIG. 1: The contributions from continuum state and dimension-six condensates for the $a_1(1260)$ -meson leading-twist DA moments $\langle \xi_{2;a_1}^{\parallel;n} \rangle_\mu$ with $n = (2, 4, 6)$ versus the Borel parameter M^2 , where all input parameters are set to the central values.

as $f_{D^0} = f_{D^+} = 0.210 \pm 0.012$ GeV, $f_{a_1}^{\parallel} = 0.238 \pm 0.010$ GeV [41]. The current-quark-mass for the light quark are $m_u = 2.16^{+0.49}_{-0.26}$ MeV and $m_d = 4.67^{+0.48}_{-0.17}$ MeV at scale $\mu = 2$ GeV. Meanwhile, the typical scale in this paper is $\mu_k = (m_D^2 - m_c^2)^{1/2} \approx 1.4$ GeV. In addition, we also need to know the values of the non-perturbative vacuum condensates up to dimension-six.

$$\begin{aligned}
 \kappa &= 0.74 \pm 0.03 \\
 \langle \alpha_s G^2 \rangle &= 0.038 \pm 0.011 \text{ GeV}^4 \\
 \langle g_s^3 f G^3 \rangle &= 0.045 \pm 0.007 \text{ GeV}^6 \\
 \langle g_s \bar{q}q \rangle^2 &= (2.082^{+0.734}_{-0.697}) \times 10^{-3} \text{ GeV}^6 \\
 \langle g_s^2 \bar{q}q \rangle^2 &= (7.420^{+2.614}_{-2.483}) \times 10^{-3} \text{ GeV}^6 \\
 \langle q\bar{q} \rangle &= (-2.417^{+0.227}_{-0.114}) \times 10^{-2} \text{ GeV}^3 \\
 \langle g_s \bar{q}\sigma T G q \rangle &= (-1.934^{+0.188}_{-0.103}) \times 10^{-2} \text{ GeV}^5 \quad (39)
 \end{aligned}$$

All the input parameters in BFTSR, i.e. the quark mass and vacuum condensates are running from initial scale μ_0 to the special scale μ_k within the renormalization group equations (RGE) given by Refs. [41–44].

B. Determination for the moments of $a_1(1260)$ -meson longitudinal twist-2 LCDA

The significant parameters for BFTSR of this calculation are the continuum threshold s_0 and Borel parameter M^2 (or Borel Window), which should satisfy the following criteria

- The continuum contributions are less than 30% of the total results;
- the contributions from the dimension-six condensates do not exceed 5%;
- The continuum threshold s_0 should close to the squared mass of the first excited state of $a_1(1260)$ -meson.

- Determining continuum threshold s_0 setting 0th-order of Gegenbauer moment into 1, i.e. $\langle \xi_{2;a_1}^{\parallel;0} \rangle_\mu = 1$.
- We require the variations of the $\langle \xi_{2;a_1}^{\parallel;n} \rangle_\mu$ within the Borel window be less than 10%.

Based on the third and fourth item of criteria, one can take the squared mass of the excited state of $a_1(1260)$ -meson, i.e. $a_1(1640)$ for $s_0 = 2.6 \pm 0.4$ GeV. For the first three order of the Gegenbauer moments $\langle \xi_{2;a_1}^{\parallel;n} \rangle_\mu$ with $n = (2, 4, 6)$, we listed the reasonable Borel windows and values of $\langle \xi_{2;a_1}^{\parallel;n} \rangle_\mu$ satisfied the above criteria in Table I. In which, the continuum contributions are less than (20%, 25%, 30%) for $n = (2, 4, 6)$, respectively, and dimension-six contributions are less than 5% for all the order of $\langle \xi_{2;a_1}^{\parallel;n} \rangle_\mu$.

Meanwhile, the continuum and dimension-six condensates contributions of the $\langle \xi_{2;a_1}^{\parallel;n} \rangle_\mu$ with $n = (2, 4, 6)$ versus the Borel parameter M^2 are shown in Fig. 1. In which the Borel windows are represented in the shaded region. In order to provide a deep insight into the flatness of the DA moments versus the Borel parameters M^2 , we present the first three curves for moments of the $a_1(1260)$ -meson twist-2 LCDA i.e. $\langle \xi_{2;a_1}^{\parallel;n} \rangle_\mu$ with $n = (2, 4, 6)$ within total uncertainties in Fig. 2 respectively. The determined Borel window in $M^2 \in [1.0, 5.5]$ GeV², within this range the moments changed less than 10% for the total result in there Borel window respectively. By taking all uncertainty sources into consideration and adopting the RGE of moments mentioned in the above subsection, We obtain $\langle \xi_{2;a_1}^{\parallel;n} \rangle_{\mu_0}$ at initial scale

$$\begin{aligned}
 \langle \xi_{2;a_1}^{\parallel;2} \rangle_{\mu_0} &= 0.210 \pm 0.018 \\
 \langle \xi_{2;a_1}^{\parallel;4} \rangle_{\mu_0} &= 0.091 \pm 0.007 \\
 \langle \xi_{2;a_1}^{\parallel;6} \rangle_{\mu_0} &= 0.052 \pm 0.004 \quad (40)
 \end{aligned}$$

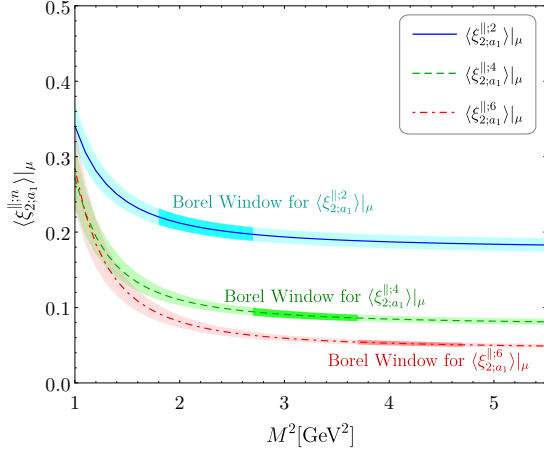


FIG. 2: The first three moments $\langle \xi_{2;a_1}^{\parallel;n} \rangle_\mu$ with $n = (2, 4, 6)$ versus the Borel parameter M^2 . The solid and dotted lines represent the central values and the shaded areas represent their errors, respectively.

By taking the squared average of all uncertainty sources into consideration and making use of the relations between Gegenbauer moments $a_{2;a_1}^{\parallel;n}(\mu_0)$ and the DA moments $\langle \xi_{2;a_1}^{\parallel;n} \rangle_{\mu_0}$, i.e. Eq. (19), we obtain the first three order $a_{2;a_1}^{\parallel;n}(\mu_0)$

$$\begin{aligned} a_{2;a_1}^{\parallel;2}(\mu_0) &= 0.030 \pm 0.054 \\ a_{2;a_1}^{\parallel;4}(\mu_0) &= -0.014 \pm 0.051 \\ a_{2;a_1}^{\parallel;6}(\mu_0) &= 0.051 \pm 0.069 \end{aligned} \quad (41)$$

Our Gegenbauer moments for the second order have agreement with the Yang's predictions [11, 12], i.e. $a_{2;a_1}^{\parallel;2}(\mu_0 = 1\text{GeV}) = -0.02 \pm 0.02$ within errors. Here, we also provide the fourth and 6th-order values firstly. Then, after taking the Gegenbauer moments $a_{2;a_1}^{\parallel;n}(\mu)$ up to 6th-order into conformal expansion with Gegenbauer polynomial Eq. (1), we present curves of $a_1(1260)$ -meson twist-2 LCDA for central value in Fig. 3. As a comparison, we also present the QCDSR result [11, 12] and asymmetry form with $\phi_{2;a_1}^{\parallel}(x) = 6x\bar{x}$. Our prediction is tend to double-peak behavior. To have a look at the evolution of $a_1(1260)$ -meson LCDA $\phi_{2;a_1}^{\parallel}(x, \mu_0)$ with increased order of $a_{2;a_1}^{\parallel;n}(\mu_0)$, the evolution curves are given in Fig. 4. When we take $n = 2$ and 4 the behavior of LCDA are closely to the asymptotic form, and the larger shake is coming from 6th-order of LCDA moment.

Other two-particle Fock state twist-3 and twist-4 LCDAs $\phi_{3;a_1}^\perp(x)$, $\psi_{3;a_1}^\perp(x)$ and $\psi_{4;a_1}^\perp(x)$ are defined as follows

$$\phi_{3;a_1}^\perp(x) = \frac{1}{2} \left[\int_0^x \frac{dv}{v} \phi_{2;a_1}^\parallel(v) + \int_x^1 \frac{dv}{v} \phi_{2;a_1}^\parallel(v) \right], \quad (42)$$

$$\psi_{3;a_1}^\perp(x) = 2\bar{x} \int_0^x \frac{dv}{v} \phi_{2;a_1}^\parallel(v) + 2x \int_x^1 \frac{dv}{v} \phi_{2;a_1}^\parallel(v), \quad (43)$$

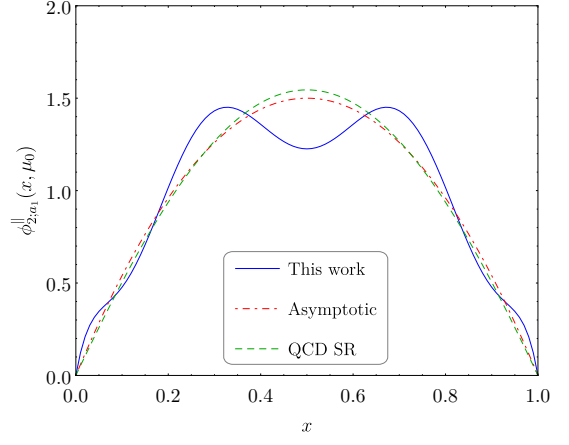


FIG. 3: The $a_1(1260)$ -meson longitudinal twist-2 LCDA $\phi_{2;a_1}^{\parallel}(x, \mu_0)$ predicted from the BFTSR. As a comparison, the QCDSR [11, 12] and asymptotic results are also present.

$$\psi_{4;a_1}^{\parallel}(x) = 6x\bar{x} + (1 - 3\xi^2) \left[\frac{1}{7} a_{2;a_1}^{\parallel;n} - \frac{20}{3} \frac{f_{3;a_1}^A}{f_{a_1}^{\parallel} m_{a_1}} \right], \quad (44)$$

where $f_{3;a_1}^A = 0.0012$ [12], $\phi_{3;a_1}^\perp(x)$ and $\psi_{3;a_1}^\perp(x)$ are related to the twist-2 LCDA by Wandzura-Wliczek approximation relations [11]. In order to evolve the hadronic parameters in $a_1(1260)$ -meson twist-2, 3, 4 LCDAs from initial factorization scale to any other scale especial for typical scale μ_k , the renormalization group equation should be used, which have the form

$$c_i(\mu_k) = L^{\gamma_{c_i}/\beta_0} c_i(\mu_0) \quad (45)$$

where $L = \alpha_s(\mu_k)/\alpha_s(\mu_0)$, $\beta_0 = 11 - 2/3n_f$, and the one-loop anomalous dimensions γ_{c_i} can be seen in our

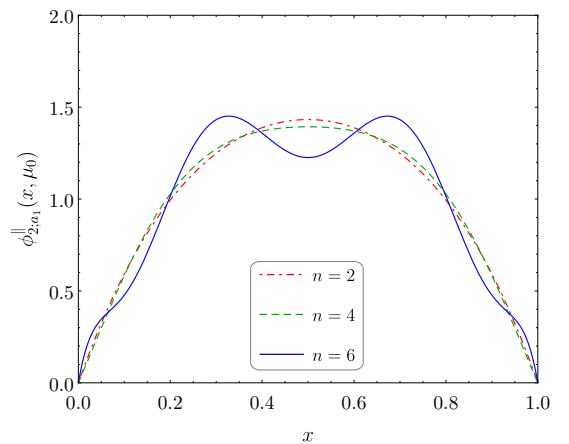


FIG. 4: The $a_1(1260)$ -meson longitudinal twist-2 LCDA $\phi_{2;a_1}^{\parallel}(x, \mu_0)$ predicted from the BFTSR by using the Gegenbauer moments up to 2th, 4th and 6th-order levels, respectively.

TABLE II: The TFFs of $D \rightarrow a_1(1260)$, i.e. $A(0), V_1(0), V_2(0), V_0(0)$ at the large recoil point $q^2 = 0$. As a comparison, we also present the prediction for various methods.

Method	$A(0)$	$V_1(0)$	$V_2(0)$	$V_0(0)$
This work	$0.130^{+0.013}_{-0.015}$	$1.899^{+0.119}_{-0.127}$	$0.211^{+0.018}_{-0.020}$	$0.235^{+0.026}_{-0.025}$
LCSR-I [45]	0.07 ± 0.05	0.37 ± 0.01	-0.03 ± 0.02	0.15 ± 0.05
LCSR-II [46]	$0.34^{+0.03}_{-0.04}$	$2.63^{+0.20}_{-0.21}$	$0.34^{+0.03}_{-0.04}$	$0.24^{+0.00}_{-0.01}$
3PSR [47]	0.09	0.77	-0.01	0.19
CLFQM [7]	0.20	1.54	0.06	0.31
CLFQM [48]	$0.19^{+0.00}_{-0.01}$	$1.51^{+0.00}_{-0.04}$	$0.05^{+0.01}_{-0.00}$	$0.32^{+0.00}_{-0.00}$

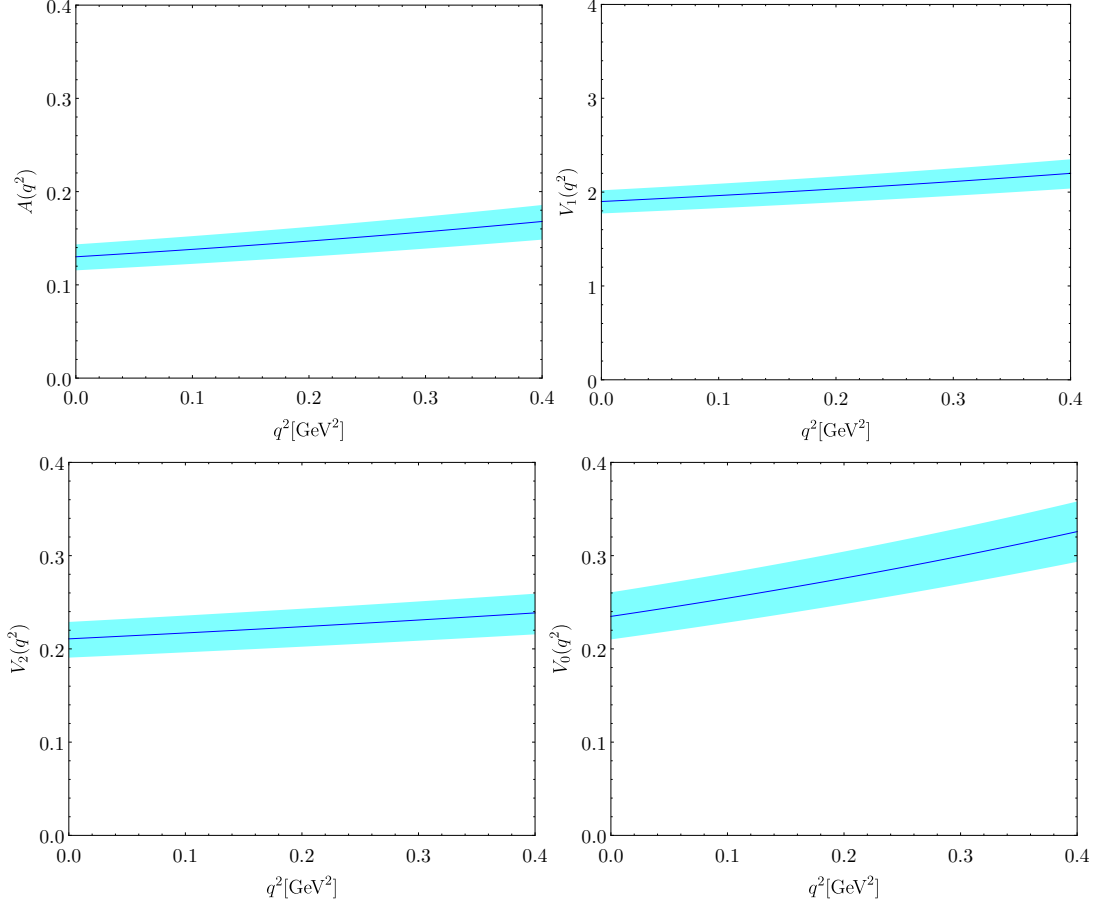


FIG. 5: The extrapolated LCSR predictions for the $D^{0(+)} \rightarrow a_1^{-(0)} e^+ \nu_e$ TFFs $A(q^2), V_1(q^2), V_2(q^2), V_0(q^2)$, the shaded bands corresponds to the uncertainties from theoretical input parameters.

previous work [49]. Taken the hadronic parameters at initial scale μ_0 , and employing the renormalization function Eq. (45), one can be obtained the corresponding values at the typical scale μ_k .

C. The $D \rightarrow a_1(1260)$ TFFs and observable for semileptonic decay $D \rightarrow a_1(1260) \ell^+ \nu_\ell$

In order to determine the continuum threshold s_0 and Borel parameter M^2 for the $D^{0(+)} \rightarrow a_1^{-(0)} \ell^+ \nu_\ell$ TFFs LCSR, i.e. Eq. (33)-(36). One can follow the four criteria

- The continuum contributions are less than 30% of the dispersion relation;
- the contributions from the twist-4 LCDAs do not

exceed 5%;

- We require the variations of the TFFs within the Borel window be less than 10%.
- The continuum threshold s_0 should close to the squared mass of the first excited state of D -meson.

According the fourth item of the criteria, the continuum thresholds of the TFFs should be taken near the squared mass of the excited state of D -meson, i.e. $D_1(2420)$. In this paper, we mainly take the following values

$$\begin{aligned} s_0^A &= 6.5 \pm 0.3 \text{ GeV}^2 \\ s_0^{V_1} &= 5.8 \pm 0.3 \text{ GeV}^2 \\ s_0^{V_2} &= 6.0 \pm 0.3 \text{ GeV}^2 \\ s_0^{V_0} &= 6.0 \pm 0.3 \text{ GeV}^2 \end{aligned} \quad (46)$$

Then, after followed the above criteria, one can determine the Borel windows for each TFFs, which are $M_A^2 = 4.0 \pm 0.3 \text{ GeV}^2$, $M_{V_1}^2 = 5.0 \pm 0.3 \text{ GeV}^2$, $M_{V_2}^2 = 5.0 \pm 0.3 \text{ GeV}^2$ and $M_{V_0}^2 = 5.0 \pm 0.3 \text{ GeV}^2$, respectively. After determining the Borel parameters and continuum thresholds, we can obtain the $D \rightarrow a_1$ TFFs at the large recoil region $q^2 \rightarrow 0 \text{ GeV}^2$ with the uncertainties are squared averages of all the mentioned error sources for the LCSR approach, which are listed in Table II. As a comparison, the predictions from various approaches are presented, i.e. the LCSR-I, II [45, 46], 3PSR [47] and CLFQM [7, 48], respectively. Our predictions are somewhere between the LCSR-I and LCSR-II, that is, larger than the LCSR-I but smaller than LCSR-II. At the same time, it can be found that there are certain differences between our results and those of other groups.

Theoretically, the squared momentum transfer of LCSR approach for $D \rightarrow a_1(1260)$ TFFs are applicable in low and intermediate q^2 -regions, i.e. $q^2 \in [0, 0.28] \text{ GeV}^2$, which is still have discrepancy with the physically allowable region $m_\ell^2 \leq (m_D - m_{a_1})^2 \approx 0.4 \text{ GeV}^2$. So one can extrapolate these TFFs to whole q^2 -regions via converging simplified series expansion (SSE) [52]

$$F_i(q^2) = \frac{1}{P_i(q^2)} \sum_k \alpha_k [z(q^2) - z(0)]^k. \quad (47)$$

In which, the $z(t)$ is the function

$$z(t) = \frac{\sqrt{t_+ - t} - \sqrt{t_+ - t_0}}{\sqrt{t_+ - t} + \sqrt{t_+ - t_0}} \quad (48)$$

where $t_\pm = (m_D \pm m_{a_1})^2$, $t_0 = t_+(1 - \sqrt{1 - t_-/t_+})$, and the $F_i(q^2)$ are the TFFs $A(q^2)$ and $V_{0,1,2}(q^2)$, respectively. The $P_i(q^2) = (1 - q^2/m_{R,i}^2)$ is a simple pole corresponding to the first resonance in the spectrum.

$$\Delta = \frac{\sum_t |F_i(t) - F_i^{\text{fit}}(t)|}{\sum_t |F_i(t)|} \times 100 \quad (49)$$

TABLE III: The fitting parameters $\alpha_{1,2}$ for the TFFs $A(q^2), V_1(q^2), V_2(q^2), V_0(q^2)$ where all input parameters are set to be their central values.

	$A(q^2)$	$V_1(q^2)$	$V_2(q^2)$	$V_0(q^2)$
α_1	-1.465	-2.174	-0.024	-4.229
α_2	26.160	205.321	1.063	47.274
Δ	0.003%	0.002%	0.000%	0.004%

where $t \in [0, 1/40, \dots, 40/40] \times 0.28 \text{ GeV}^2$. The fitting parameters α_i for TFFs and the quality of fit Δ are listed in Table III. From which, the Δ of $D \rightarrow a_1(1260)$ TFFs are less than 0.004%. Then, we present the extrapolating TFFs $A(q^2), V_{0,1,2}(q^2)$ within errors in Fig. 5.

Furthermore, the $|V_{cd}|$ -independence longitudinal and transverse differential decay width $d\Gamma_{L,T}$ and total widths $d\Gamma_{\text{total}} = d\Gamma_L + d\Gamma_T$ of $D \rightarrow a_1(1260)\ell^+\nu_\ell$ can be obtained according to Eqs. (37) and (38), which are shown in Fig. 6. From which, the left panel stands for the $D \rightarrow a_1(1260)e^+\nu_e$ channel and right one $D \rightarrow a_1(1260)\nu^+\bar{\nu}_\nu$. As a comparison, we also present other LCSR prediction [46]. The figure shown that, the contribution of decay widths mainly come from the longitudinal parts for small q^2 -region, and transverse parts for large q^2 -region. The three curves of our predictions are convergence to 0 when the squared momentum transfer tend to small recoil region, i.e. $q^2 \rightsquigarrow (m_D - m_{a_1})^2 \approx 0.4 \text{ GeV}^2$, which have the same behavior with most of other semileptonic decay processes such as final state involving $\pi, K, \rho, K^*, D, \dots$. This is different with other LCSR predictions for this processes from Ref. [46].

Finally, by taking the lifetimes initial state D^0, D^+ -mesons, $\tau_{D^0} = (0.410 \pm 0.015) \text{ ps}$, $\tau_{D^+} = (1.040 \pm 0.007) \text{ ps}$ from PDG [40], we can get the branching fractions for the two different semileptonic decay channels $D^0 \rightarrow a_1^-\ell^+\nu_\ell$ and $D^+ \rightarrow a_1^0\ell^+\nu_\ell$, which are presented in Table IV. Meanwhile, other theoretical predictions such as LCSR-I, II [45, 46] and CLFQM [50] are also given as a comparison. Our results have agreement with other predictions which are in order of 10^{-5} . At present, $D^{0(+)} \rightarrow a_1^{-(0)}(1260)\ell^+\nu_\ell$ has not been measured by the experimental groups. In 2020, the BESIII collaboration measured $D^{0(+)} \rightarrow b_1^{-(0)}e^+\nu_e$ decay processes and provided the upper limits on the product branching fractions, which are $\mathcal{B}(D^0 \rightarrow b_1^-(1235)e^+\nu_e) \cdot \mathcal{B}(b_1(1235)^- \rightarrow \omega\pi^-) < 1.12 \times 10^{-4}$ and $\mathcal{B}(D^+ \rightarrow b_1^0(1235)e^+\nu_e) \cdot \mathcal{B}(b_1(1235)^0 \rightarrow \omega\pi^0) < 1.75 \times 10^{-4}$ [51]. In which the $\mathcal{B}(b_1(1235)^{0(-)} \rightarrow \omega\pi^{0(-)}) = 1$ [46] and one can get the branching fraction for $D \rightarrow b_1(1235)e^+\nu_e$ directly. Furthermore, the branching fractions of $D \rightarrow a_1(1260)\ell^+\nu_\ell$ of this work satisfies this upper limit, i.e 10^{-4} . It is hoped that the semileptonic decay $D \rightarrow a_1(1260)\ell\nu_\ell$ can be measured by experimental collaboration in the near future.

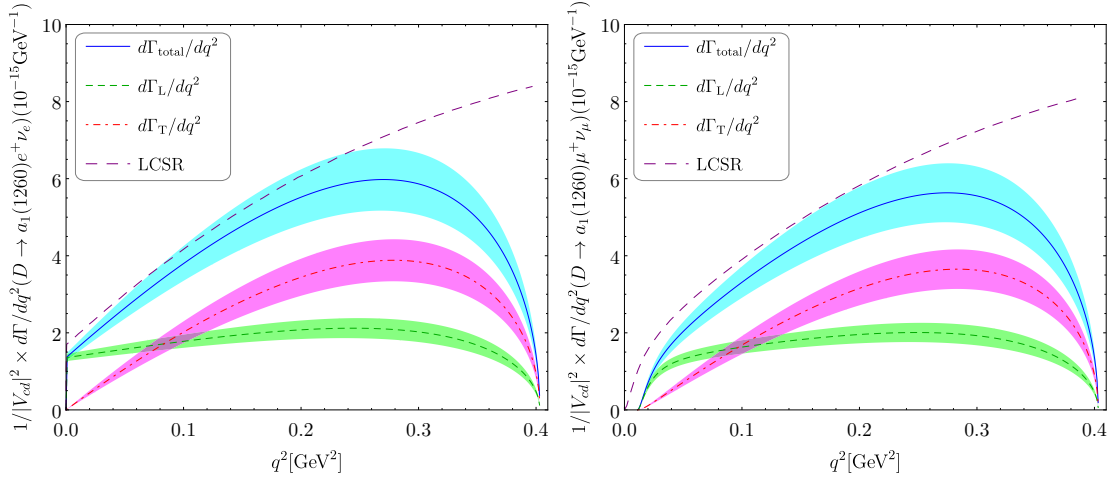


FIG. 6: Decay width for the $D \rightarrow a_1(1260)\ell^+\nu_\ell$ versus q^2 by using the chiral LCSR for the TFFs and by adopting the BFTSR for the twist-2 LCDA. As a comparison, we also present the other LCSR results from Ref. [46].

TABLE IV: Branching fractions of $D \rightarrow a_1(1260)\ell^+\nu_\ell$. The errors are squared averages of all the mentioned error sources. As a comparison, we also present the prediction for various methods.

Method	$\mathcal{B}(D^0 \rightarrow a_1^-(1260)e^+\nu_e)$	$\mathcal{B}(D^+ \rightarrow a_1^0(1260)e^+\nu_e)$	$\mathcal{B}(D^0 \rightarrow a_1^-(1260)\mu^+\nu_\mu)$	$\mathcal{B}(D^+ \rightarrow a_1^0(1260)\mu^+\nu_\mu)$
This work	$(5.421_{-0.697}^{+0.702}) \times 10^{-5}$	$(6.875_{-0.884}^{+0.890}) \times 10^{-5}$	$(4.864_{-0.641}^{+0.647}) \times 10^{-5}$	$(6.169_{-0.813}^{+0.821}) \times 10^{-5}$
LCSR-I [45]	$(3.58 \pm 0.52) \times 10^{-5}$	$(4.73 \pm 0.63) \times 10^{-5}$		
LCSR-II [46]	6.90×10^{-5}	9.38×10^{-5}	6.27×10^{-5}	8.52×10^{-5}
CLFQM [50]	4.1×10^{-5}		3.6×10^{-5}	

IV. SUMMARY

In the present paper, we have calculated the longitudinal distribution amplitude $\phi_{2;a_1}^\parallel$ of the $a_1(1260)$ -meson by using the BFTSR approach up to NLO QCD corrections for the perturbative part and up to dimension-six condensates for the non-perturbative part. The Borel window of the BFTSR is fixed by requiring the contribution of the continuum states to be less than 30% and the contribution of the dimension-six contribution to be less than 5%, which are shown in Table I and Fig. 1. The moments of LCDA and the Gegenbauer moments up to 6th-order have been listed in Eq. (40) and Eq. (41) respectively. Fig. 4 shows that $\phi_{2;a_1}^\parallel(x, \mu_0)$ tends to double-peak behavior by using more and more known Gegenbauer moments. Moreover, by using the derived LCDA, we have calculated the $D \rightarrow a_1(1260)$ TFFs $A(q^2)$, $V_{0,1,2}(q^2)$ by using the LCSR approach within a left-hand current up to twist-4 order, whose extrapolated behavior in whole region can be found in Fig. 5. Furthermore, the $|V_{cd}|$ -independence differential decay width of semileptonic decay $D \rightarrow a_1(1260)\ell^+\nu_\ell$ with $\ell = (e, \mu)$ have been given in Fig. 6, and the branching fractions for $D^{0(+)} \rightarrow a_1^{-(0)}\ell^+\nu_\ell$ have been given in Table IV. The branching fractions are of order 10^{-5} , which is close to the present experimental upper limit. It is hoped that

the decay $D \rightarrow a_1(1260)\ell\nu_\ell$ can be observed in near future, which inversely could provide a (potential) helpful test of QCD sum rules approach.

V. ACKNOWLEDGMENTS

Hai-Bing Fu would like to thank the Institute of Theoretical Physics in Chongqing University for kind hospitality. This work was supported in part by the National Natural Science Foundation of China under Grant No.11765007, No.11947406, No.11625520, No.11875122, and No.12047564, the Project of Guizhou Provincial Department of Science and Technology under Grant No.KY[2019]1171, and No.ZK[2021]024, the Project of Guizhou Provincial Department of Education under Grant No.KY[2021]030 and No.KY[2021]003, the Fundamental Research Funds for the Central Universities under Grant No.2020CQJQY-Z003, and the Project of Guizhou Minzu University under Grant No. GZMU[2019]YB19.

Appendix A: Matrix element for $a_1(1260)$ -meson LCDAs

The matrix elements of definition $a_1(1260)$ twist-2, 3, 4 LCDAs [11, 13]

$$\langle a_1(p, \lambda) | \bar{d}(x) \gamma_\mu u(0) | 0 \rangle = -\frac{im_{a_1} f_{a_1}^\parallel}{4} \epsilon^{\mu\nu\alpha\beta} e_\nu^{*(\lambda)} x_\alpha p_\beta \times \int_0^1 du e^{iup \cdot x} \psi_{3;a_1}^\perp(u) \quad (\text{A1})$$

$$\langle a_1(p, \lambda) | \bar{d}(x) \gamma_\mu \gamma_5 u(0) | 0 \rangle = im_{a_1} f_{a_1}^\parallel \int_0^1 du e^{iup \cdot x} \times \left\{ \frac{e^{*(\lambda)} \cdot x}{p \cdot x} p_\mu \phi_{2;a_1}^\parallel(u) + e_{\perp\mu}^{*(\lambda)} \phi_{3;a_1}^\perp(u) - \frac{e^{*(\lambda)} \cdot x}{2(p \cdot x)^2} m_{a_1}^2 x_\mu \psi_{4;a_1}^\parallel \right\} \quad (\text{A2})$$

$$\langle a_1(p, \lambda) | \bar{d}(x) \gamma_\alpha \gamma_5 g_s G_{\mu\nu}(\nu x) u(0) | 0 \rangle = -p_\alpha \left[p_\mu e_{\perp\nu}^{*(\lambda)} \right.$$

$$\left. - p_\nu e_{\perp\mu}^{*(\lambda)} \right] f_{3;a_1}^A \Phi_{3;a_1}^\parallel(v, p \cdot x) \quad (\text{A3})$$

$$\langle a_1(p, \lambda) | \bar{d}(x) \gamma_\alpha g_s \tilde{G}_{\mu\nu}(\nu x) u(0) | 0 \rangle = ip_\alpha \left[p_\mu e_{\perp\nu}^{*(\lambda)} - p_\nu e_{\perp\mu}^{*(\lambda)} \right] f_{3;a_1}^V \tilde{\Phi}_{3;a_1}^\parallel(v, p \cdot x) \quad (\text{A4})$$

Where $\tilde{G}_{\mu\nu} = \frac{1}{2} \epsilon_{\mu\nu\alpha\beta} G^{\alpha\beta}$, the value of coupling constants $f_{3;a_1}^A$ and $f_{3;a_1}^V$ for $a_1(1260)$ -meson at $\mu = 1\text{GeV}$. In which, we have set

$$e_{\perp\mu}^{*(\lambda)} = e_\mu^{*(\lambda)} - \frac{e^{*(\lambda)} \cdot x}{p \cdot x} \left(p_\mu - \frac{m_{a_1}^2}{2p \cdot x} x_\mu \right) \\ K(v, p \cdot x) = \int_0^1 d\alpha_1 d\alpha_2 d\alpha_3 \delta(1 - \alpha_1 - \alpha_2 - \alpha_3) \times e^{-i(\alpha_2 - \alpha_1 + v\alpha_3)p \cdot x} K(\alpha_i). \quad (\text{A5})$$

-
- [1] B. Aubert *et al.* [BABAR Collaboration], Observation of B^0 meson decays to $a_1^\pm(1260)\pi^\mp$, [hep-ex/0408021].
- [2] B. Aubert *et al.* [BABAR Collaboration], Observation of B^0 meson decay to $a_1^\pm(1260)\pi^\mp$, *Phys. Rev. Lett.* **97** (2006) 051802.
- [3] B. Aubert *et al.* [BABAR Collaboration], Measurements of CP-Violating asymmetries in $B^0 \rightarrow a_1^\pm(1260)\pi^\mp$ decays, *Phys. Rev. Lett.* **98** (2007) 181803.
- [4] K. Abe *et al.* [Belle Collaboration], Observation of $B^0 \rightarrow a_1^\pm(1260)\pi^\mp$, [hep-ex/0507096].
- [5] K. Abe *et al.* [Belle Collaboration], Measurement of the branching fraction for $B^0 \rightarrow a_1^\pm(1260)\pi^\mp$ with 535 million $B\bar{B}$ pairs, [arXiv:0706.3279].
- [6] T. M. Aliev and M. Savci, Semileptonic $B \rightarrow a_1$ lepton neutrino decay in QCD, *Phys. Lett. B* **456** (1999) 256-263.
- [7] H. Y. Cheng, C. K. Chua and C. W. Hwang, Covariant light front approach for s wave and p wave mesons: Its application to decay constants and form-factors, *Phys. Rev. D* **69** (2004) 074025.
- [8] A. Deandrea, R. Gatto, G. Nardulli and A. D. Polosa, Semileptonic $B \rightarrow \rho$ and $B \rightarrow a_1$ transitions in a quark - meson model, *Phys. Rev. D* **59** (1999) 074012.
- [9] Z. G. Wang, Analysis of the $B \rightarrow a_1(1260)$ form-factors with light-cone QCD sum rules, *Phys. Lett. B* **666** (2008) 477-482.
- [10] Y. J. Sun, Z. G. Wang and T. Huang, $B \rightarrow A$ Transitions in the Light-Cone QCD Sum Rules with the Chiral current, *Chin. Phys. C* **36** (2012) 1046-1054.
- [11] K. C. Yang, Light-cone distribution amplitudes of axial-vector mesons, *Nucl. Phys. B* **776** (2007) 187-257.
- [12] K. C. Yang, Form-Factors of $B_{(u,d,s)}$ Decays into P-Wave Axial-Vector Mesons in the Light-Cone Sum Rule Approach, *Phys. Rev. D* **78** (2008) 034018.
- [13] S. Momeni, R. Khosravi and F. Falahati, Flavor changing neutral current transition of B to a_1 with light-cone sum rules, *Phys. Rev. D* **95** (2017) 016009.
- [14] W. Wang, R. H. Li and C. D. Lu, Radiative charmless $B_{(s)} \rightarrow V\gamma$ and $B_{(s)} \rightarrow A\gamma$ decays in pQCD approach, [arXiv:0711.0432].
- [15] R. H. Li, C. D. Lu and W. Wang, Transition form factors of B decays into p-wave axial-vector mesons in the perturbative QCD approach, *Phys. Rev. D* **79** (2009) 034014.
- [16] X. Liu and Z. J. Xiao, $B \rightarrow a_1(1260)a_1(1260)$ and $b_1(1235)b_1(1235)$ decays in the perturbative QCD approach, *Phys. Rev. D* **86** (2012) 074016.
- [17] R. Khosravi, Form factors and branching ratios of the FCNC $B \rightarrow a_1 \ell^+ \ell^-$ decays, *Eur. Phys. J. C* **75** (2015) 220.
- [18] T. Huang and Z. Huang, Quantum Chromodynamics in Background Fields, *Phys. Rev. D* **39**, (1989) 1213.
- [19] T. Zhong, X. G. Wu, Z. G. Wang, T. Huang, H. B. Fu and H. Y. Han, Revisiting the pion leading-twist distribution amplitude within the QCD background field theory, *Phys. Rev. D* **90** (2014) 016004.
- [20] H. B. Fu, X. G. Wu, W. Cheng and T. Zhong, ρ -meson longitudinal leading-twist distribution amplitude within QCD background field theory, *Phys. Rev. D* **94** (2016) 074004.
- [21] H. B. Fu, L. Zeng, W. Cheng, X. G. Wu and T. Zhong, Longitudinal leading-twist distribution amplitude of the J/ψ meson within the background field theory, *Phys. Rev. D* **97** (2018) 074025.
- [22] T. Zhong, X. G. Wu and T. Huang, Heavy pseudoscalar leading-twist distribution amplitudes within QCD theory in background fields, *Eur. Phys. J. C* **75** (2015) 45.
- [23] T. Zhong, X. G. Wu, T. Huang and H. B. Fu, Heavy pseudoscalar twist-3 distribution amplitudes within QCD theory in background fields, *Eur. Phys. J. C* **76** (2016) 509.
- [24] T. Zhong, X. G. Wu, J. W. Zhang, Y. Q. Tang and Z. Y. Fang, New results on pionic twist-3 distribution amplitudes within the QCD sum rules, *Phys. Rev. D* **83** (2011) 036002.
- [25] H. Y. Han, X. G. Wu, H. B. Fu, Q. L. Zhang and T. Zhong, Twist-3 distribution amplitudes of scalar mesons within the QCD sum rules and its

- application to the $B \rightarrow S$ transition form factors, *Eur. Phys. J. A* **49** (2013) 78.
- [26] T. Huang, X. H. Wu and M. Z. Zhou, Twist three distribute amplitudes of the pion in QCD sum rules, *Phys. Rev. D* **70** (2004) 014013.
- [27] T. Huang, M. Z. Zhou and X. H. Wu, Twist-3 distribution amplitudes of the pion and kaon from the QCD sum rules, *Eur. Phys. J. C* **42** (2005) 271.
- [28] T. Zhong, X. G. Wu, H. Y. Han, Q. L. Liao, H. B. Fu and Z. Y. Fang, Revisiting the twist-3 distribution amplitudes of K -meson within the QCD background field approach, *Commun. Theor. Phys.* **58** (2012) 261.
- [29] T. Zhong, Y. Zhang, X. G. Wu, H. B. Fu and T. Huang, The ratio $\mathcal{R}(D)$ and the D -meson distribution amplitude, *Eur. Phys. J. C* **78** (2018) 937.
- [30] D. D. Hu, H. B. Fu, T. Zhong, L. Zeng, W. Cheng and X. G. Wu, η -meson leading-twist distribution amplitude within QCD sum rule approach and its application to the semi-leptonic decay $D_s^+ \rightarrow \eta \ell^+ \nu_\ell$, [[arXiv:2102.05293](#)].
- [31] Y. M. Makeenko and A. A. Migdal, Exact Equation for the Loop Average in Multicolor QCD, *Phys. Lett. B* **88** (1979) 135.
- [32] M. A. Shifman, A. I. Vainshtein, M. B. Voloshin and V. I. Zakharov, η_c Puzzle in Quantum Chromodynamics, *Phys. Lett. B* **77** (1978) 80.
- [33] P. Ball, V. M. Braun, Y. Koike and K. Tanaka, Higher twist distribution amplitudes of vector mesons in QCD: Formalism and twist-2 distributions, *Nucl. Phys. B* **529** (1998) 323-382.
- [34] M. A. Shifman, A. I. Vainshtein and V. I. Zakharov, QCD and Resonance Physics: Applications, *Nucl. Phys. B* **147** (1979) 448.
- [35] J. Govaerts, F. de Viron, D. Gusbin and J. Weyers, Exotic mesons from QCD sum rules, *Phys. Lett. B* **128** (1983) 262.
- [36] V. A. Novikov, M. A. Shifman, A. I. Vainshtein and V. I. Zakharov, Calculations in External Fields in Quantum Chromodynamics. Technical Review, *Fortsch. Phys.* **32** (1984) 585.
- [37] W. Hubschmid and S. Mallik, Operator expansion at short distance in QCD, *Nucl. Phys. B* **207** (1982) 29-42.
- [38] P. Colangelo and A. Khodjamirian, QCD sum rules, a modern perspective, (2000).
- [39] T. Zhong, Z. H. Zhu, H. B. Fu, X. G. Wu and T. Huang, An improved light-cone harmonic oscillator model for the pionic leading-twist distribution amplitude, [[arXiv:2102.03989](#)].
- [40] P. A. Zyla *et al.* [Particle Data Group], Review of Particle Physics, *PTEP* **2020** (2020) 083C01.
- [41] H. Mutuk, Mass Spectra and Decay Constants of Heavy-Light Mesons: A Case Study of QCD Sum Rules and Quark Model, *Adv. High Energy Phys.* **2018**,(2018) 8095653.
- [42] K. C. Yang, W. Y. P. Hwang, E. M. Henley and L. S. Kisslinger, QCD sum rules and neutron proton mass difference, *Phys. Rev. D* **47** (1993) 3001.
- [43] W. Y. P. Hwang and K. C. Yang, QCD sum rules: $\Delta - N$ and $\Sigma^0 - \Lambda$ mass splittings, *Phys. Rev. D* **49** (1994) 460.
- [44] C. D. Lü, Y. M. Wang and H. Zou, Twist-3 distribution amplitudes of scalar mesons from QCD sum rules, *Phys. Rev. D* **75** (2007) 056001.
- [45] S. Momeni and R. Khosravi, Semileptonic $D_{(s)} \rightarrow A \ell^+ \nu$ and nonleptonic $D \rightarrow K_1(1270, 1400) \pi$ decays in LCSR, *J. Phys. G* **46** (2019) 105006.
- [46] Q. Huang, Y. J. Sun, D. Gao, G. H. Zhao, B. Wang and W. Hong, Study of form factors and branching ratios for $D \rightarrow S, A \ell \bar{\nu}_\ell$ with light-cone sum rules, [[arXiv:2102.12241](#)].
- [47] Y. Zuo, Y. Hu, L. He, W. Yang, Y. Chen and Y. Hao, $D \rightarrow a_1, f_1$ transition form factors and semileptonic decays via 3-point QCD sum rules, *Int. J. Mod. Phys. A* **31** (2016) 1650116.
- [48] R. C. Verma, Decay constants and form factors of s-wave and p-wave mesons in the covariant light-front quark model, *J. Phys. G* **39** (2012) 025005.
- [49] H. B. Fu, W. Cheng, R. Y. Zhou and L. Zeng, $D \rightarrow P(\pi, K)$ helicity form factors within light-cone sum rule approach, *Chin. Phys. C* **44** (2020) 113103.
- [50] W. Wang and Z. X. Zhao, Production of a_1 in heavy meson decays, *Eur. Phys. J. C* **76** (2016) 59.
- [51] M. Ablikim *et al.* [BESIII Collaboration], Search for the semileptonic decay $D^{0(+)} \rightarrow b_1(1235)^{-(0)} e^+ \nu_e$, *Phys. Rev. D* **102** (2020) 112005.
- [52] A. Bharucha, T. Feldmann and M. Wick, Theoretical and phenomenological constraints on form factors for radiative and semi-leptonic B -meson decays, *JHEP* **1009** (2010) 090.